ACS APPLIED MATERIALS & INTERFACES

Research Article

www.acsami.org

# Enhancement of the Fill Factor through an Increase of the Crystallinity in Fullerene-Based Small-Molecule Organic Photovoltaic Cells

Min-Soo Choi,[†] Tae-Min Kim,[†] Hyun-Sub Shim,[†] Beom-Soo Kim,[†] Hyo Jung Kim,[‡] and Jang-Joo Kim*,[†]

[†]Department of Materials Science and Engineering, Seoul National University, Seoul 151-744, South Korea

[‡]Department of Organic Material Science and Engineering, College of Engineering, Pusan National University, Busan 609-735, South Korea

Supporting Information

**ABSTRACT:** We report that the crystallinity of $C_{70}$ is improved significantly if CuI is used as a templating layer, leading to remarkable enhancement of hole mobilities from $8.32 \times 10^{-6}$ to $3.26 \times 10^{-5}$ $cm^2/(V\ s)$. As a result, the use of the templating layer in $C_{70}$-based solar cells with low donor concentration resulted in significant improvement of the fill factor from 0.51 to 0.57 and the power conversion efficiency from 5.56% to 6.23% under simulated AM 1.5G, 1 sun irradiation. This result demonstrates that the CuI templating layer is effective at improving the crystallinity of the fullerene derivatives as well as the donor materials.

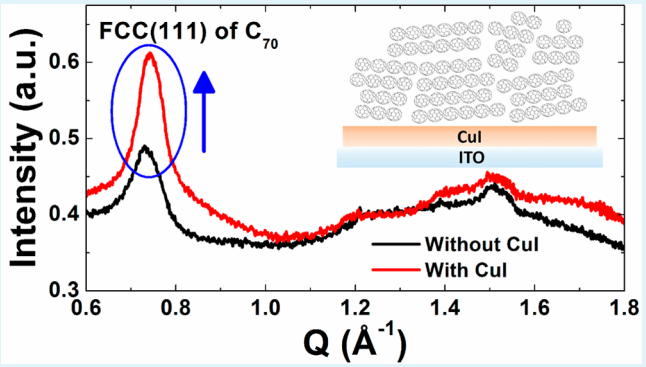


**KEYWORDS:** *organic photovoltaic, templating layer, copper iodide, $C_{70}$, low donor concentration*

## 1. INTRODUCTION

Small-molecule organic photovoltaic cells (OPVs) have been highlighted because of their advantages of ease of processing, low cost, high purity, flexibility, and easiness to control their molecular properties by synthesis.[1,2] For highly efficient OPVs, fullerene derivatives are used as common acceptor materials because of high electron mobility[3] and their energy levels to form charge-transfer states with various donor materials.[4−9] Among them, $C_{70}$ as well as $C_{60}$ is known to form intermolecular charge-transfer excitons between the molecules in solid films. The formation of a charge-transfer exciton results in extra absorption from 400 to 700 nm, leading to more photocurrent generation.[10,11] In addition, the charge-transfer exciton can be dissociated easily by doping a small amount of donor materials, such as 1,1-bis[4-bis(4-methylphenyl)-aminophenyl]cyclohexane (TAPC),[12] tetraphenyldibenzoperi-flanthene,[13,14] and tris[4-(5-phenylthiophen-2-yl)phenyl]-amine.[15] With this property of $C_{70}$, OPVs with low donor concentration have been highlighted showing high short-circuit current density ($J_{SC}$) and open-circuit voltage ($V_{OC}$).[12−15] In this system, the electron mobility is high enough to extract the electrons because of the large portion of fullerene, which possesses an n-type property.[16−19] However, the hole mobility is relatively low, which causes a reduction of the fill factor (FF) due to the unbalanced electron and hole mobilities.[20,21] The increase of the hole mobility is a critical factor in obtaining a higher power conversion efficiency (PCE) with improving FF.

In organic films, the optical and electrical properties are significantly influenced by the molecular orientation, crystal structure, and crystallinity. The transition dipole moment has an intimate relationship with the molecular orientation, and control of the molecular orientation can result in a remarkable increase of the photocurrent coming from the increased absorption coefficient.[22−27] The charge mobilities in a molecular film are also influenced by the molecular orientation, crystallinity, and crystal structure. High crystalline films possess low defect density, leading to high charge mobility.[28−31] There has been a large effort to increase the crystallinity, especially in planar heterojunction solar cells. Among them, the use of a templating layer has been widely studied as an effective way, and CuI is known as an effective templating material for organic donor materials to improve the PCE combined with controlling the crystal structure and molecular orientation for organic materials.[23−27] Unfortunately, however, there are few reports on control of the crystallinity of fullerene derivatives using a templating layer. Pentacene[29,30] and diindenoperylene[31,32] were reported to increase the crystallinity of $C_{60}$ for n-type transistors. However, their high highest occupied molecular orbital (HOMO) energy may reduce $V_{OC}$ if adopted in solar cells.

**Received:** February 6, 2015
**Accepted:** April 15, 2015
**Published:** April 15, 2015





DOI: 10.1021/acsami.5b01166
ACS Appl. Mater. Interfaces 2015, 7, 9134−9138

In this study, we report that the crystallinity of $C_{70}$ is improved significantly if CuI is used as the templating layer, leading to remarkable enhancement of hole mobilities in the layers. The grazing-incident X-ray diffraction (GIXRD) patterns show significant enhancement of the crystallinity of a (111)-oriented FCC phase of $C_{70}$ when CuI is inserted as the templating layer on an indium−tin oxide (ITO) substrate. The use of the templating layer also causes an increase of the hole mobility from $8.32 \times 10^{-6}$ to $3.26 \times 10^{-5}$ $cm^2/(V\ s)$. As a result, the use of the templating layer in $C_{70}$-based solar cells with low donor concentration resulted in a significant improvement of the FF from 0.51 to 0.57 and the PCE from 5.56% to 6.23% under simulated AM 1.5G, 1 sun irradiation.

## 2. EXPERIMENTAL SECTION

The ITO-coated glass substrates were cleaned with acetone and isopropyl alcohol and exposed to UV−$O_3$ for 10 min before use. $ReO_3$ and CuI were used as interfacial layers and deposited using thermal evaporation onto the substrate at a base pressure of ca. $10^{-7}$ Torr with a rate of 0.1 Å/s. TAPC and $C_{70}$ were also deposited using thermal evaporation onto the substrate with different rates of 0.1 and 1.9 Å/s in order to form a 5% TAPC-doped $C_{70}$ layer. The exciton blocking layer, bathocuproine (BCP), and aluminum metal cathode were deposited with rates of 1.0 and 4.0 Å/s, respectively. All of the layers were successively evaporated without breaking the vacuum, and all devices were encapsulated in $N_2$ ambient before photocurrent measurements. The photovoltaic properties of the devices were measured with an AM 1.5G 100 $mW/cm^2$ solar simulator (300 W Oriel 69911A) light source and a source measurement unit (Keithley 237). The measurement setup was calibrated with a National Renewable Energy Laboratory certified reference silicon solar cell covered with a KG-5 filter before measurement. More than six devices with the cell area of $2 \times 2$ $mm^2$ were averaged to calculate the cell performance. The crystalline structures were investigated by synchrotron X-ray diffraction measurements at the 5A X-ray scattering beamline for materials science at Pohang Light Source II (PLS-II). The X-ray wavelength was 1.072 Å (11.57 keV) at an incident angle of 0.2°.

## 3. RESULTS AND DISCUSSION

Figure 1 shows the GIXRD patterns of the $C_{70}$ films doped with 5% TAPC (active layers). The organic films are deposited on the ITO substrate covered with a 1-nm-thick $ReO_3$ layer for GIXRD samples because active layers of the solar cells are grown on the substrate. The diffraction pattern of the 50-nm-thick $C_{70}$ film doped with 5% TAPC shows four peaks, which

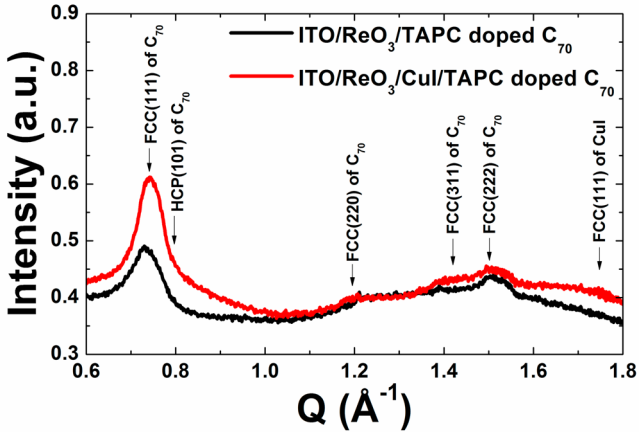


**Figure 1.** GIXRD patterns of 5% TAPC-doped $C_{70}$ films. The film structures are ITO (150 nm)/$ReO_3$ (1 nm)/with or without CuI (1 nm)/5% TAPC-doped $C_{70}$ (50 nm), and the incident angle is 0.2°.

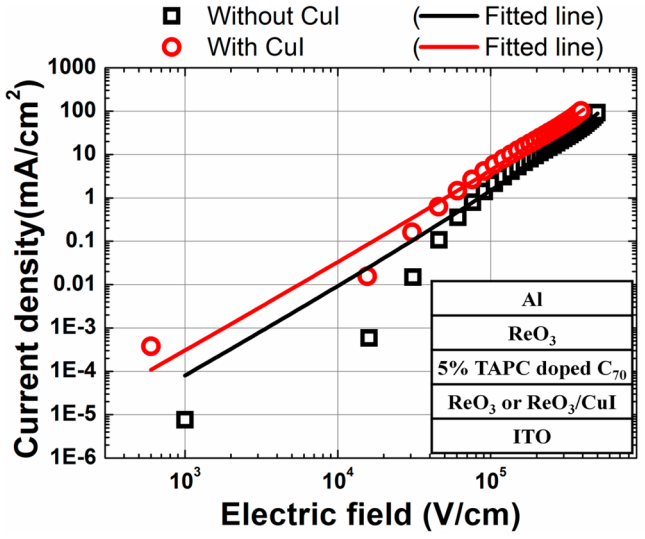


**Figure 2.** Current densities against the applied voltage for hole-only devices of the 5% TAPC-doped $C_{70}$ film to extract hole mobilities. Device structures are ITO (150 nm)/$ReO_3$ (1 nm)/with or without CuI (1 nm)/5% TAPC-doped $C_{70}$ (500 nm)/$ReO_3$ (5 nm)/Al (100 nm). The open symbols are experimental $J-V$ characteristics for the single carrier devices, while the solid lines are fits using the SCLC model.

can be assigned as the (111)-oriented ($Q$ = 0.74 $Å^{-1}$), the (220)-oriented ($Q$ = 1.20 $Å^{-1}$), the (311)-oriented ($Q$ = 1.42 $Å^{-1}$), and the (222)-oriented ($Q$ = 1.50 $Å^{-1}$) FCC phases of the $C_{70}$, respectively.[33] The (111) and (222) peaks have high peak intensities compared to other peaks. When the 5% TAPC-doped $C_{70}$ film is grown on the 1-nm-thick CuI deposited on a $ReO_3$/ITO substrate, the intensity of the (111) peak is remarkably increased compared to the film grown on $ReO_3$, indicating that the crystallinity increases significantly with CuI. The pattern also shows a shoulder at $Q$ = 0.8 $Å^{-1}$, which is not shown from the sample without CuI in addition to the (111)-oriented FCC phase of CuI.[34] The shoulder can be assigned as the (101)-oriented HCP phase of $C_{70}$ originating from the stacking fault of the (111)-oriented FCC phase of $C_{70}$.[35] The peak of the stacking fault is very broad compared to other peaks because of the anisotropic property of $C_{70}$.[36] Including the stacking fault, the crystallinity of the FCC phase was increased remarkably, especially the (111)-oriented FCC phase. The results clearly indicate that the templating layer significantly improves the crystallinity of the $C_{70}$ film doped with 5% TAPC on the ITO substrate. Interestingly enough, the morphology did not change much even though the crystallinity in the grains increased significantly by introducing the CuI layer (Figure S4 in the Supporting Information, SI).

Hole mobilities in the active layer were extracted from the current density−voltage ($J-V$) curves of hole-only devices in the space-charge-limited current (SCLC; Figure 2). The device structures are ITO (150 nm)/$ReO_3$ (1 nm)/with or without CuI (1 nm)/5% TAPC-doped $C_{70}$ (500 nm)/$ReO_3$ (5 nm)/Al (100 nm). The $ReO_3$ layers were used in the devices to form an ohmic contact for hole injection at the anode side and to block electron injection at the cathode side. The built-in potential in the device was expected to be negligible because of the $ReO_3$ layers. In contrast, the built-in potential in the active layer cannot be negligible when the 1-nm-thick CuI layer was inserted between $ReO_3$ and the active layer because CuI has a different work function from $ReO_3$, leading to modification of


DOI: 10.1021/acsami.5b01166
ACS Appl. Mater. Interfaces 2015, 7, 9134−9138

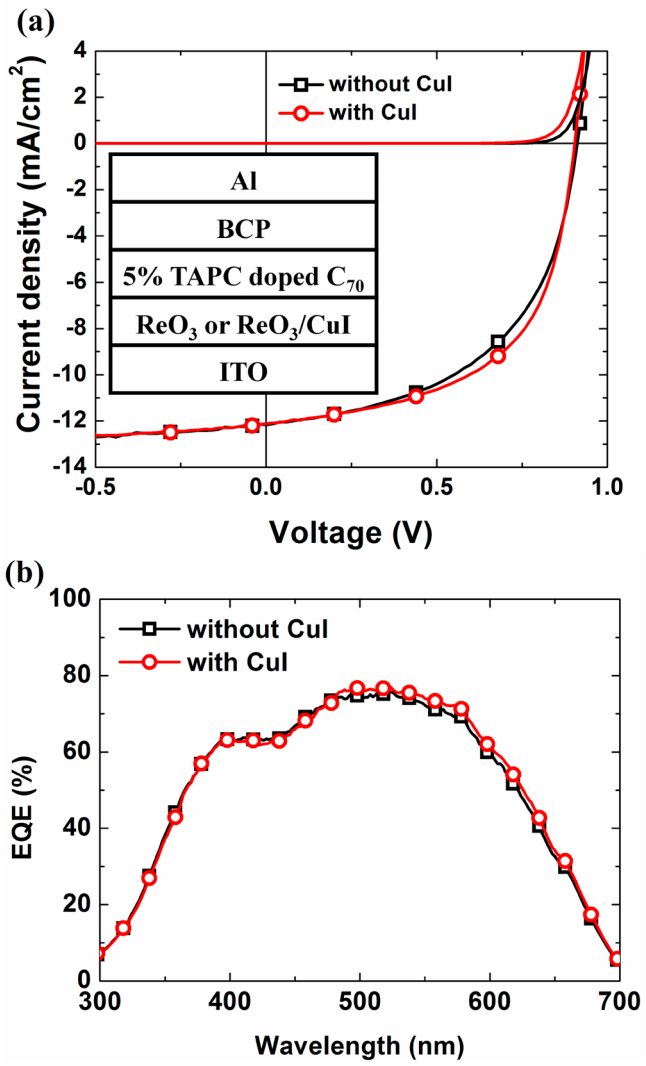


**Figure 3.** (a) $J-V$ characteristics with and without the CuI templating layer under AM 1.5G illumination. The device structures are ITO/$ReO_3$ (1 nm)/with or without CuI (1 nm)/5% TAPC-doped $C_{70}$ (60 nm)/BCP (8 nm)/Al (100 nm). (b) IPCE data for the devices.

the energy level alignment. The built-in potential of the device with the CuI layer was estimated from the difference of the built-in potentials of the devices of ITO (150 nm)/$ReO_3$ (1 nm)/with or without CuI (1 nm)/$C_{70}$ (60 nm)/BCP (8 nm)/Al (100 nm). The built-in potentials of the devices with and without the CuI layer were calculated as 0.986 and 0.763, respectively, from analysis of the capacitance−voltage characteristics using the Mott−Schottky relationship shown in Figure S1 in the SI.[37,38] On the basis of measurements, the hole-only device with the CuI layer was assumed to have a built-in potential of −0.22 V. With consideration of the built-in field, hole mobilities in the active layer from SCLC fitting increased from $8.32 \times 10^{-6}$ to $3.26 \times 10^{-5}$ cm$^2$/(V s) when the 1-nm-thick CuI layer was inserted between $ReO_3$ and the active layer. The increased hole mobility was consistent with enhancement in the crystallinity of the TAPC-doped $C_{70}$ film when deposited on CuI. The electron mobility also increased from $3.4 \times 10^{-5}$ to $5.3 \times 10^{-5}$ cm$^2$/(V s) upon insertion of the CuI layer, which was measured by the time-of-flight method using the structures of ITO (150 nm)/with or without CuI (1 nm)/5% TAPC-doped $C_{70}$ (1000 nm)/Al (100 nm) shown in Figure S5 in the SI.

Figure 3a shows the $J-V$ characteristics of the OPV cells with the structure of ITO (150 nm)/$ReO_3$ (1 nm)/with or without CuI (1 nm)/5% TAPC-doped $C_{70}$ (60 nm)/BCP (8 nm)/Al (100 nm) in the dark and under illumination of an AM 1.5G 100 mW/cm$^2$ solar simulated light source. Table 1 summarizes the solar cell performance of $J_{SC}$, $V_{OC}$, FF, PCE, and the series resistance ($R_S$) obtained by fitting the dark $J-V$ curves with the Shockley diode equation. The OPV cells show the same $V_{OC}$ value of 0.91 V, because it was determined by the HOMO of TAPC and the lowest unoccupied molecular orbital (LUMO) of $C_{70}$. $J_{SC}$ of two devices also show the same value of 12.0 mA/cm$^2$ with the same absorption spectra (shown in Figure S2 in the SI). This value is close to the calculated photocurrent using the transfer matrix method and the refractive indices measured by variable-angle ellipsometry, as shown in Figure S3 in the SI. The very good match between the experimental and calculated $J_{SC}$ values indicates that the 1-nm-thick $ReO_3$ layer acts as an efficient hole extraction layer because of its high work function, leading to a large built-in field distributed in the device at short-circuit conditions. In contrast, FF increases from 51.2% to 57.1% by insertion of the CuI templating layer. It can be understood based on the electron and hole mobilities. In spite of the high electron mobility of the film, a low hole mobility of the film results in an accumulation of hole carriers in the film, leading to bimolecular recombination and reduced FF. However, the use of the CuI layer enhances the hole mobility, improves hole extraction, and reduces bimolecular recombination in the device, leading to an increase of the FF and PCE of the solar cells with low donor concentration.

The incident photon-to-electron conversion efficiencies (IPCEs) of the OPVs with and without the CuI templating layer are shown in Figure 3b. The IPCE of the device with CuI is slightly higher than that of the device without CuI in the range from 480 to 700 nm. This is due to enhanced charge extraction caused by an increase in the hole mobility. The IPCE data were used to calculate $J_{SC}$ using the AM 1.5G solar spectrum, and the calculated $J_{SC}$ values of the OPV cells with and without CuI layer were 11.7 and 11.5 mA/cm$^2$, resulting in the corrected PCEs of 6.10% and 5.36%.

## 4. CONCLUSION

The use of CuI as the templating layer in a $C_{70}$-based low-donor-concentration organic solar cell improves the FF significantly from 0.51 to 0.57 without any change in $J_{SC}$ and

**Table 1. Solar Cell Performance with and without the CuI Templating Layer**[a]

| | PCE (%) | $J_{SC}$ (mA/cm$^2$) | $V_{OC}$ (V) | FF (%) | $R_S$ (Ω cm$^2$) | $n$ | $J_S$ (mA/cm$^2$) |
|---|---|---|---|---|---|---|---|
| without CuI | 5.59 ± 0.33 | 12.0 ± 0.2 | 0.91 ± 0.01 | 51.2 ± 2.5 | 2.17 | 1.51 | $6.59 \times 10^{-11}$ |
| with CuI | 6.23 ± 0.04 | 12.0 ± 0.2 | 0.91 ± 0.02 | 57.1 ± 0.8 | 2.08 | 1.47 | $5.51 \times 10^{-11}$ |

[a]The series resistance ($R_S$), ideality factor ($n$), and dark saturation current density ($J_S$) are obtained by fitting the dark $J-V$ curve with the Shockley diode equation.



DOI: 10.1021/acsami.5b01166
ACS Appl. Mater. Interfaces 2015, 7, 9134−9138

$V_{OC}$ to increase the PCE from 5.59% to 6.23%. It turned out that the improvement comes from the increased crystallinity of $C_{70}$ in the active layer and from an increase in the hole mobility to get better charge extraction and less electron−hole recombination in the active layer. This result clearly demonstrates that not only the crystallinity of the donor materials but also the crystallinity of fullerene derivatives is important in organic solar cells especially in low-donor-concentration organic solar cells, and the use of CuI as a templating layer is effective to increase the crystallinity of fullerene derivatives as well as the donor materials.

## ■ ASSOCIATED CONTENT

### Supporting Information

Capacitance−voltage characteristics of Schottky solar cells, calculated $J_{SC}$ of the solar cell by a transfer matrix method, absorption spectra of organic films, AFM images, and transient photocurrent profiles. This material is available free of charge via the Internet at http://pubs.acs.org.

## ■ AUTHOR INFORMATION

### Corresponding Author

*E-mail: jjkim@snu.ac.kr.

### Notes

The authors declare no competing financial interest.

## ■ ACKNOWLEDGMENTS

This work (Grant 2014R1A2A1A01002030) was supported by the Midcareer Researcher Program through an National Research Foundation grant funded by the Ministry of Science, ICT and Future Planning.

## ■ REFERENCES

(1) Lin, L.-Y.; Chen, Y.-H.; Huang, Z.-Y.; Lin, H.-W.; Chou, S.-H.; Lin, F.; Chen, C.-W.; Liu, Y.-H.; Wong, K.-T. A Low-Energy-Gap Organic Dye for High-Performance Small-Molecule Organic Solar Cells. *J. Am. Chem. Soc.* **2011**, *133*, 15822−15825.

(2) Chen, Y.-H.; Lin, S.-Y.; Lu, C.-W.; Lin, F.; Huang, Z.-Y.; Lin, H.-W.; Wang, P.-H.; Liu, Y.-H.; Wong, K.-T.; Wen, J.; Miller, D. J.; Darling, S. B. Vacuum-Deposited Small-Molecule Organic Solar Cells with High Power Conversion Efficiencies by Judicious Molecular Design and Device Optimization. *J. Am. Chem. Soc.* **2012**, *134*, 13616−13623.

(3) Kobayashi, S.; Takenobu, T.; Mori, S.; Fujiwara, A.; Iwasa, Y. Fabrication and Characterization of C60 Thin-Film Transistors with High Field-Effect Mobility. *Appl. Phys. Lett.* **2003**, *82*, 4581−4583.

(4) Lof, R. W.; van Veenendaal, M. A.; Koopmans, B.; Jonkman, H. T.; Sawatzky, G. A. Band Gap, Excitons, and Coulomb Interaction in Solid C60. *Phys. Rev. Lett.* **1992**, *68*, 3924−3927.

(5) Osikowicz, W.; de Jong, M. P.; Salaneck, W. R. Formation of the Interfacial Dipole at Organic−Organic Interfaces: C60/Polymer Interfaces. *Adv. Mater.* **2007**, *19*, 4213−4217.

(6) Ohno, T. R.; Chen, Y.; Harvey, S. E.; Kroll, G. H.; Weaver, J. H. C60 Bonding and Energy-Level Alignment on Metal and Semiconductor Surface. *Phys. Rev. B* **1991**, *44*, 13747−13755.

(7) Harigaya, K. Lattice Distortion and Energy-Level Structures in Doped C60 and C70 Molecules Studied with the Extended Su-Schrieffer-Heeger Model: Polaron Excitations and Optical Absorption. *Phys. Rev. B* **1992**, *45*, 13676−13684.

(8) Saito, S.; Oshiyama, A.; Miyamoto, Y.; Hamada, N.; Sawada, S.-I. Electronic Structure of Fullerenes and Fullerides: Artificial Atoms and Their Solids. *Nanotechnology* **1992**, *3*, 167−172.

(9) Sariciftci, N. S.; Smilowitz, L.; Heeger, A. J.; Wudl, F. Photoinduced Electron Transfer from a Conducting Polymer to Buckminsterfullerene. *Science* **1992**, *258*, 1474−1476.

(10) Pope, M.; Swenberg, C. E. *Electronic Precesses of Organic Crystals and Polymers*, 2nd ed.; Oxford University Press: New York, 1999.

(11) Wang, Y. M.; Kamat, P. V.; Patterson, L. K. Aggregates of C60 and C70 Formed at the Gas−Water Interface and in DMSO/Water Mixed Solvents. A Spectral Study. *J. Phys. Chem.* **1993**, *97*, 8793−8797.

(12) Zhang, M.; Wang, H.; Tian, H.; Geng, Y.; Tang, C. W. Bulk Heterojunction Photovoltaic Cells with Low Donor Concentration. *Adv. Mater.* **2011**, *23*, 4960−4964.

(13) Xiao, X.; Zimmerman, J. D.; Lassiter, B. E.; Bergemann, K. J.; Forrest, S. R. A Hybrid Planar-Mixed tetraphenyldibenzoperiflanthene/C70 Photovoltaic Cell. *Appl. Phys. Lett.* **2013**, *102*, 073302-1−073302-4.

(14) Zheng, Y. Q.; Potscavage, W. J., Jr.; Komino, T.; Hirade, M.; Adachi, J.; Adachi, C. Highly Efficient Bulk Heterojunction Photovoltaic Cells based on C70 and tetraphenyldibenzoperiflanthene. *Appl. Phys. Lett.* **2013**, *102*, 143304-1−143304-5.

(15) Zheng, Y. Q.; Potscavage, W. J., Jr.; Komino, T.; Adachi, C. Highly Efficient Bulk Heterojunction Photovoltaic Cell based on tris[4-(5-phenylthiophen-2-yl)phenyl]amine and C70 Combined with Optimized Electron Transport Layer. *Appl. Phys. Lett.* **2013**, *102*, 153302-1−153302-4.

(16) Chen, G.; Sasabe, H.; Wang, Z.; Wang, X.-F.; Hong, Z.; Yang, Y.; Kido, J. Co-Evaporated Bulk Heterojunction Solar Cells with >6.0% Efficiency. *Adv. Mater.* **2012**, *24*, 2768−2773.

(17) Pandey, R.; Gunawan, A. A.; Mkhoyan, K. A.; Holmes, R. J. Efficient Organic Photovoltaic Cells Based on Nanocrystalline Mixtures of Boron Subphthalocyanine Chloride and C60. *Adv. Funct. Mater.* **2012**, *22*, 617−624.

(18) Kudo, K.; Saraya, T.; Kuniyoshi, S.; Tanaka, K. Electrical Characterization of C60 Evaporated Films Using MOS Structure. *Mol. Cryst. Liq. Cryst.* **1995**, *261*, 423428.

(19) Ecker, B.; Nolasco, J. C.; Pallarés, J.; Marsal, L. F.; Posdorfer, J.; Parisi, J.; Hauff, E. V. Degradation Effects Related to the Hole Transport Layer in Organic Solar Cells. *Adv. Funct. Mater.* **2011**, *21*, 2705−2711.

(20) Tress, W.; Petrich, A.; Hummert, M.; Hein, M.; Leo, K.; Riede, M. Imbalanced Mobilities causing S-shaped IV Curves in Planar Heterojunction Organic Solar Cells. *Appl. Phys. Lett.* **2011**, *98*, 063301-1−063301-3.

(21) Lee, C.-T.; Lee, C.-H. Conversion Efficiency Improvement Mechanisms of Polymer Solar Bells by Balance Electron−Hole Mobility Using Blended P3HT:PCBM:pentacene Active Layer. *Org. Electron.* **2013**, *14*, 2046−2050.

(22) Kim, H. J.; Shim, H.-S.; Kim, J. W.; Lee, H. H.; Kim, J.-J. CuI Interlayers in Lead Phthalocyanine Thin Films Enhance Near-Infrared Light Absorption. *Appl. Phys. Lett.* **2012**, *100*, 263303-1−263303-4.

(23) Shim, H.-S.; Kim, H. J.; Kim, J. W.; Kim, S.-Y.; Jeong, W.-I.; Kim, T.-M.; Kim, J.-J. Enhancement of Near-Infrared Absorption with High Fill Factor in Lead Phthalocyanine-based Organic Solar Cells. *J. Mater. Chem.* **2012**, *22*, 9077−9081.

(24) Cheng, C. H.; Wang, J.; Du, G. T.; Shi, S. H.; Du, Z. J.; Fan, Z. Q.; Bian, J. M.; Wang, M. S. Organic Solar Cells with Remarkable Enhanced Efficiency by Using a CuI Buffer to Control the Molecular Orientation and Modify the Anode. *Appl. Phys. Lett.* **2010**, *97*, 083305-1−083305-3.

(25) Kim, T.-M.; Shim, H.-S.; Choi, M.-S.; Kim, H. J.; Kim, J.-J. Multilayer Epitaxial Growth of Lead Phthalocyanine and C70 Using CuBr as a Templating Layer for Enhancing the Efficiency of Organic Photovoltaic Cells. *ACS Appl. Mater. Interfaces* **2014**, *6*, 4286−4291.

(26) Kim, T.-M.; Kim, H. J.; Shim, H.-S.; Choi, M.-S.; Kim, J. W.; Kim, J.-J. The Epitaxial Growth of Lead Phthalocyanine on Copper Halogen Compounds as the Origin of Templating Effects. *J. Mater. Chem. A* **2014**, *2*, 8730−8735.

(27) Kim, J. W.; Kim, H. J.; Kim, T.-M.; Kim, T. G.; Lee, J.-H.; Kim, J. W.; Kim, J.-J. High Performance Organic Planar Heterojunction Solar Cells by Controlling the Molecular Orientation. *Curr. Appl. Phys.* **2013**, *13*, 7−11.

(28) Singh, T. B.; Sariciftci, N. S.; Yang, H.; Yang, L.; Plochberger, P.; Sitter, H. Correlation of Crystalline and Structural Properties of C60



DOI: 10.1021/acsami.5b01166
*ACS Appl. Mater. Interfaces* 2015, 7, 9134−9138

Thin Films Grown at Various Temperature with Charge Carrier Mobility. *Appl. Phys. Lett.* **2007**, *90*, 213512-1−213512-3.
(29) Itaka, K.; Yamashiro, M.; Yamaguchi, J.; Haemori, M.; Yaginuma, S.; Matsumoto, Y.; Kondo, M.; Koinuma, H. High-Mobility C60 Field-Effect Transistors Fabricated on Molecular-Wetting Controlled Substrates. *Adv. Mater.* **2006**, *18*, 1713−1716.
(30) Zhou, J.-L.; Yu, J.-S.; Yu, X.-G.; Cai, X.-Y. A High Mobility C60 Field-Effect Transistor with an Ultrathin Pentacene Passivation Layer and Bathophenanthroline/Metal Bilayer Electrodes. *Chin. Phys. B* **2012**, *21*, 021305-1−021305-6.
(31) Yang, J.-P.; Sun, Q.-J.; Yonezawa, K.; Hinderhofer, A.; Gerlach, A.; Broch, K.; Bussolotti, F.; Gao, X.; Li, Y.; Tang, J.; Schreiber, F.; Ueno, N.; Wang, S.-D.; Kera, S. Interface Optimization Using diindenoperylene for C60 Thin Film Transistors with High Electron Mobility and Stability. *Org. Electron.* **2014**, *15*, 2749−2755.
(32) Hinderhofer, A.; Gerlach, A.; Broch, K.; Hosokai, T.; Yonezawa, K.; Kato, K.; Kera, S.; Ueno, N.; Schreiber, F. Geometric and Electronic Structure of Templated C60 on Diindenoperylene Thin Films. *J. Phys. Chem. C* **2013**, *117*, 1053−1058.
(33) Valsakumar, M. C.; Subramanian, N.; Yousuf, M.; Sahu, P. Ch.; Hariharan, Y.; Bharathi, A.; Sankara Sastry, V.; Janaki, J.; Rao, G. V. N.; Radhakrishnan, T. S.; Sundar, C. S. Crystal Structure and Disorder in Solid C70. *Phys. Rev. B* **1993**, *48*, 9080−9085.
(34) Ng, C. H. B.; Fan, W. Y. Facile Synthesis of Single-Crystalline γ-CuI Nanotetrahedrons and Their Induced Transformation to Tetrahedral CuO Nanocages. *J. Phys. Chem. C* **2007**, *111*, 9166−9171.
(35) Gong, J.; Ma, G.; Chen, G. Structural Transitions and Electrical Conductivity of C60 Films at High Temperature. *J. Mater. Res.* **1996**, *11*, 2071−2075.
(36) Guo, Y.; Karasawa, N.; Goddard, W. A. Prediction of Fullerene Packing in C60 and C70 Crystals. *Nature* **1991**, *351*, 464−467.
(37) Liu, S.-W.; Su, W.-C.; Lee, C.-C.; Cheng, C.-W.; Chou, C.-C.; Lina, C.-F. Absorbing Visible Light Materials of Subphthalocyanine and C70 for Efficient Planar-Mixed Organic Photovoltaic Devices. *J. Electrochem. Soc.* **2013**, *160*, G14−G18.
(38) Bisquert, J.; Garcia-Belmonte, G.; Munar, A.; Sessolo, M.; Soriano, A.; Bolink, H. J. Band Unpinning and Photovoltaic Model for P3HT:PCBM Organic Bulk Heterojunctions under Illumination. *Chem. Phys. Lett.* **2008**, *465*, 57−62.


DOI: 10.1021/acsami.5b01166
*ACS Appl. Mater. Interfaces* 2015, 7, 9134−9138